Improving the coherence time of superconducting coplanar resonators

H. Wang, M. Hofheinz, J. Wenner, M. Ansmann, R. C. Bialczak, M. Lenander, Erik Lucero, M. Neeley, A. D. O'Connell, D. Sank, M. Weides, A. N. Cleland, and John M. Martinis[a)]
Department of Physics, University of California, Santa Barbara, California 93106, USA

The quality factor and energy decay time of superconducting resonators have been measured as a function of material, geometry, and magnetic field. Once the dissipation of trapped magnetic vortices is minimized, we identify a power-dependent decay mechanism that is consistent with the surface two-level state model. A wide gap between the center conductor and the ground plane, as well as use of the superconductor Re instead of Al, are shown to decrease loss. We also demonstrate that classical measurements of resonator quality factor at low excitation power are consistent with single-photon decay time measured using qubit-resonator swap experiments. © 2009 American Institute of Physics. [doi:10.1063/1.3273372]

Superconducting coplanar resonators have many important applications such as photon detection[1] and quantum computation,[2,3] and recently have been used to host arbitrary photon states generated by coupling to qubits.[4–6] A key parameter limiting the resonator performance in a qubit-resonator coupling experiment is the energy relaxation time T_1, while dephasing is relatively unimportant.[5] Resonator performance and its limiting factors have been studied through classical measurements of the quality factor in several interesting experiments.[7–13] However, various loss mechanisms remain to be clarified and minimized.

Here we show how several previously untested loss mechanisms can be eliminated or optimized to reach a measured quality factor Q_m in the 200 000 to 400 000 range at low power. The internal quality factor Q_i can be higher after subtracting Q_c, the limiting quality factor due to electrical loading through coupling capacitors. We identify an important loss mechanism, which is likely from surface two-level state (TLS) defects. Finally, we show how relatively simple quality factor measurements, when taken at low power, can be used to predict the energy decay time of resonators at the single photon level.

For this work, we measured various half-wavelength ($\lambda/2$) and quarter-wavelength ($\lambda/4$) coplanar resonators, as described in Fig. 1 and Table I. Aluminum (Al) films were sputter deposited and etched with a Cl_2/BCl_3-based reactive ion etch (RIE), whereas Rhenium (Re) was electron-beam evaporated in a molecular beam epitaxy system using a substrate temperature of 850 °C and etched with SF_6/Ar-based RIE. The films were fabricated as part of a multilayer process to enable testing with qubits. Q_m of the resonators was determined in an adiabatic demagnetization refrigerator using a vector network analyzer, with approximately 35 dB attenuation on the input and 10 dB on the output of the resonator box between 100 mK and 4 K.[14] Q_c's estimated from the $|S_{21}|$ calibration were ~400 000 (~1 000 000) for $\lambda/2$ ($\lambda/4$) resonators but were not subtracted from Q_m.

For all the resonators we observed an increase in Q_m as the measurement power increased and temperature T decreased. The T dependence is shown in Fig. 2(a) for repre-

sentative resonators, taken with high excitation power. To avoid complications due to different geometries, we base most of the discussion on $\lambda/4$ resonators as they share a similar shape. The decrease in Q_m with increasing temperature is consistent with quasiparticle dissipation. In Fig. 2(b), the fractional change in the resonance frequency $\Delta f_0/f_0$ tends to level off around 100 mK, and its magnitude scales inversely with the center trace width, w_c, which is consistent with the kinetic inductance theory.[15] The monotonic variation of resonance frequency [Fig. 2(b), inset], similar to that of the NbTiN resonator,[10] is slightly different than previous studies on Nb, Ta, and Al resonators,[8,10–12] which showed a slight downturn at temperatures below $T_c/10$ due to TLS.

In Figs. 3(a) and 3(b) we plot Q_m versus excitation voltage. Note that Q_m increases by a factor of 2 to 3 for an
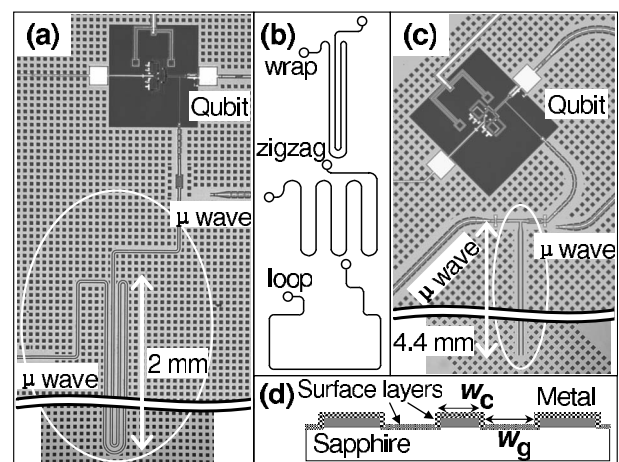

FIG. 1. Description of resonator devices. (a) Photomicrograph of a wrap-geometry $\lambda/2$ resonator (circled) coupled to a qubit through a few femto-farad capacitor and a microwave drive through a sub femtofarad capacitor for T_1 measurement. Resonator for Q measurement is coupled to a second microwave drive through a sub femtofarad capacitor and disconnected from the qubit. (b) Illustrations (not to scale) of different geometries used for $\lambda/2$ resonators. The total length of coplanar lines are all about 8.8 mm. (c) A straight $\lambda/4$ resonator (circled) coupled to a qubit and a microwave drive for T_1. Resonator for Q is coupled to a second microwave drive and disconnected from the qubit. (d) Cross-section of the coplanar resonator showing the center trace width w_c, and the gap separation w_g between the center trace and the ground plane.

a)Electronic mail: martinis@physics.ucsb.edu.

TABLE I. Resonator parameters. The thickness of the metal films are 110–130 nm, and widths w_c and w_g were chosen to give a 50 Ω characteristic impedance, except for the $w_g = 12$ μm resonator. Q_m is quoted at low power, $V_{rms} \sim 10^{-5}$ V, and T_1 is determined via qubit-resonator swap experiments.

Metal, geometry	w_c (μm)	w_g (μm)	f_0 (GHz)	Q_m (k)	$Q_m/2\pi f_0$ (μs)	T_1 (μs)
Re, $\lambda/2$, loop	5	2	6.3	100	2.5	2.0
Re, $\lambda/2$, zigzag	5	2	6.6	40	1.0	1.0
Re, $\lambda/2$, wrap	5	2	6.6	90	2.2	3.5
Re, $\lambda/2$, zigzag	10	4	6.8	200	4.7	5.1
Al, $\lambda/2$, loop	5	2	6.7	60		
Al, $\lambda/2$, wrap	5	2	7.0	60		
Al, $\lambda/2$, zigzag	10	4	7.1	110		
Re, $\lambda/4$, straight	5	2	6.8	150		
Re, $\lambda/4$, straight	8	3.2	6.9	210		
Re, $\lambda/4$, straight	16	6.4	7.0	330		
Re, $\lambda/4$, straight	16	12	7.0	230	5.3	6.4
Al, $\lambda/4$, straight	5	2	7.0	72		
Al, $\lambda/4$, straight	8	3.2	7.0	110		
Al, $\lambda/4$, straight	16	6.4	7.1	170		

increase in power by a factor $\sim 10^4$. An increase is naturally explained by TLS loss, which scales with the electric field E as $1/\sqrt{1+E^2/E_s^2}$, where E_s is a saturation field for TLS loss. For a coplanar resonator with a nonuniform field distribution,[14] numerical calculations indicate that TLS loss at the surface of the metal can be well approximated by $(1/Q_{TLS})/\sqrt{1+(V_{rms}/V_s')^\beta}$, where V_{rms} is the root-mean-squared voltage on the center conductor, $V_s' \sim w_g E_s$, and $\beta \approx 1.6$.[16]

To explain the weak power dependence, we postulate an additional loss mechanism $1/Q_0$ that is independent of power in the experimentally examined power range. We find the data can be well fit with parameters Q_0 and Q_{TLS} that are plotted in Fig. 3(c), along with their dependence on the coplanar gap width w_g. We find Q_{TLS} for both the Re and Al resonators increases with larger w_g, and the TLS loss from Re is approximately three times lower than for Al, suggesting that TLS loss comes from the metal surface of the reso-

nator. Q_{TLS} scales as w_g^α for $\alpha \sim 1$ [solid lines in Fig. 3(c)].[8] Additionally, the magnitude of Q_{TLS} is explained by a 3 nm thick oxide on the Al metal with a loss tangent 0.01, reasonably close to previous findings.[14,17] We expect Re, which is much less reactive than Al, to have a thinner oxide, although both films may be covered by a few monolayer thick film of water and/or stray contaminants. We also find that Re and Al have similar background loss Q_0, which could arise from coupling, radiation, nonequilibrium quasiparticles, magnetic vortices, and possibly other unknown mechanisms.[16]
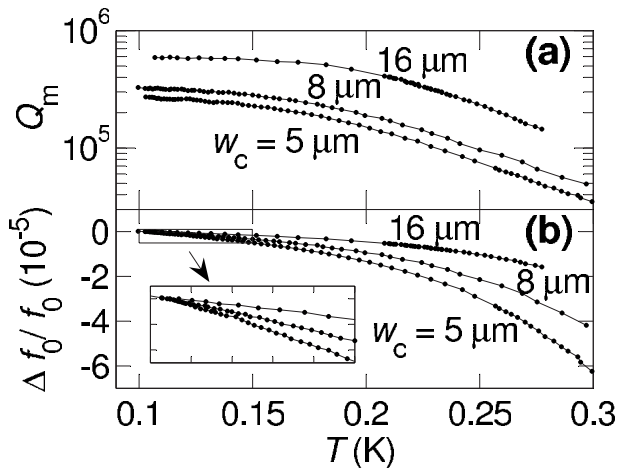

FIG. 2. (a) Plot of Q_m vs temperature at high excitation power ($V_{rms} \sim 10^{-2}$ V) for Re $\lambda/4$ resonators with different center-trace widths w_c, as indicated. (b) Fractional variations of the resonance frequency $\Delta f_0/f_0$ vs temperature for resonators shown in (a). The variation scales inversely with w_c, characteristic of kinetic inductance. Inset shows the low temperature regime where a monotonic change of f_0 is observed down to the lowest temperature. Lines are guides to the eye.
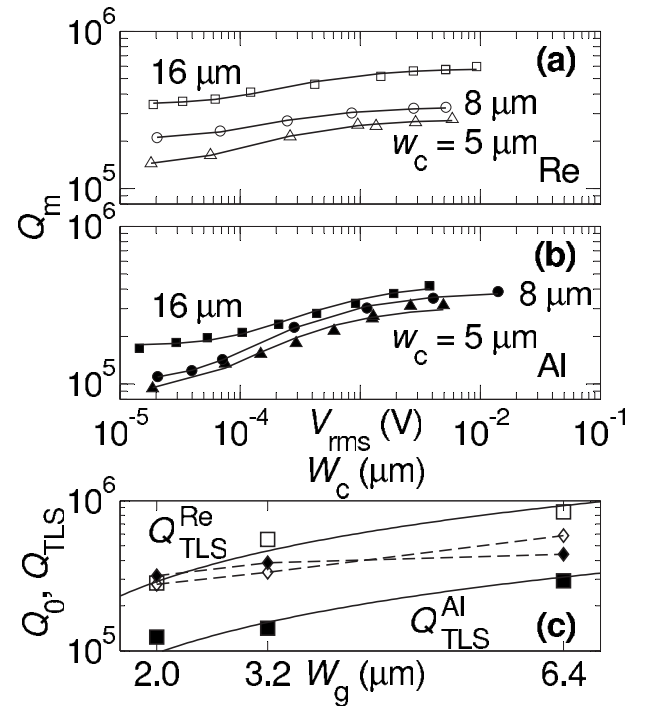
FIG. 3. (a) Q_m vs resonator voltage V_{rms} (with $V_{rms}^2 \propto$ power) for Re $\lambda/4$ resonators of different gap widths w_g. Lines are fits to the data. (b) Same as (a), but for Al resonators. Note that Q_m for Al is systematically lower than for Re. (c) Results from a fit to a power-independent Q_0 (diamonds) and power-dependent Q_{TLS} (squares), vs w_g. Open (filled) symbols are for Re (Al). Corresponding trace width w_c is shown on top scale. Solid lines are fits using $Q_{TLS} \propto w_g$ from surface TLS loss. Dashed lines are guide to the eye.
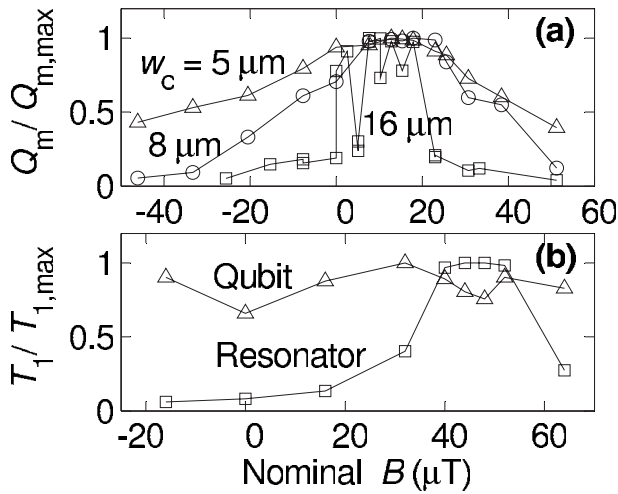
FIG. 4. (a) Normalized Q_m vs the applied cooling field B for Re $\lambda/4$ resonators of different trace widths w_c. (b) Normalized T_1 vs the applied field, as measured with a qubit, for a Re $\lambda/4$ resonator with $w_c=16$ μm and $w_g=12$ μm. Data for the resonator and qubit is shown. Lines are drawn as a guide to the eye.

Although a wider gap w_g suppresses TLS loss, care must be taken not to introduce loss from trapped vortices, created when the film is cooled through its superconducting transition.[18,19] The effect of the applied field on Q_m is shown in Fig. 4(a), which is consistent with the requirement that the cooling field $B_c \lesssim \Phi_0/w_c^2$ must be reduced as the center trace widens, where Φ_0 is the magnetic flux quantum. This condition indicates a preference for narrow trace widths and holes in the ground plane. We note that using μ-metal shielding does not guarantee low magnetic fields at the sample because components, such as microwave connectors with plated Ni, may introduce stray magnetic fields. We found that all data had to be taken after optimizing the applied field for maximum Q_m.

The effects of different resonator geometries are listed in Table I. We do not find a significant systematic dependence, suggesting that radiation effects are small with these devices.

Does Q_m actually predict the energy decay rate of a single photon? In Table I we compare the resonator decay time $Q_m/2\pi f_0$, determined at low power, with the measured single-photon decay time T_1 from the qubit-resonator swap experiment.[5] Good agreement is found for the subset of our data where resonators and qubit-resonator devices were fabricated on the same wafer. The single-photon T_1 measurements provide the most stringent measure since elevated temperatures or powers typically increase the apparent Q_m in resonators.

In conclusion, we have identified several loss mechanisms in superconducting coplanar resonators. The layout geometry has been determined to be unimportant at present loss levels but loss from trapped superconducting vortices must be minimized by using narrow traces and cooling through the transition temperature in an optimized magnetic field. We have found an important decay mechanism explainable by the surface TLS, which can be reduced by designing coplanar resonators with wide gaps and by using superconductors with little surface oxide, such as Re.

[1] P. K. Day, H. G. LeDuc, B. A. Mazin, A. Vayonakis, and J. Zmuidzinas, Nature (London) **425**, 817 (2003).

[2] A. Wallraff, D. I. Schuster, A. Blais, L. Frunzio, R.-S. Huang, J. Majer, S. Kumar, S. M. Girvin, and R. J. Schoelkopf, Nature (London) **431**, 162 (2004).

[3] M. A. Sillanpää, J. I. Park, and R. W. Simmonds, Nature (London) **449**, 438 (2007).

[4] M. Hofheinz, E. M. Weig, M. Ansmann, R. C. Bialczak, E. Lucero, M. Neeley, A. D. O'Connell, H. Wang, J. M. Martinis, and A. N. Cleland, Nature (London) **454**, 310 (2008).

[5] H. Wang, M. Hofheinz, M. Ansmann, R. C. Bialczak, E. Lucero, M. Neeley, A. D. O'Connell, D. Sank, J. Wenner, A. N. Cleland, and J. M. Martinis, Phys. Rev. Lett. **101**, 240401 (2008).

[6] M. Hofheinz, H. Wang, M. Ansmann, R. C. Bialczak, E. Lucero, M. Neeley, A. D. O'Connell, D. Sank, J. Wenner, J. M. Martinis, and A. N. Cleland, Nature (London) **459**, 546 (2009).

[7] J. Gao, J. Zmuidzinas, B. A. Mazin, H. G. Leduc, and P. K. Day, Appl. Phys. Lett. **90**, 102507 (2007).

[8] J. Gao, M. Daal, A. Vayonakis, S. Kumar, J. Zmuidzinas, B. Sadoulet, B. A. Mazin, P. K. Day, and H. G. Leduc, Appl. Phys. Lett. **92**, 152505 (2008).

[9] J. Gao, M. Daal, J. M. Martinis, A. Vayonakis, J. Zmuidzinas, B. Sadoulet, B. A. Mazin, P. K. Day, and H. G. Leduc, Appl. Phys. Lett. **92**, 212504 (2008).

[10] R. Barends, H. L. Hortensius, T. Zijlstra, J. J. A. Baselmans, S. J. C. Yates, J. R. Gao, and T. M. Klapwijk, Appl. Phys. Lett. **92**, 223502 (2008).

[11] J. Baselmans, S. J. C. Yates, R. Barends, Y. J. Y. Lankwarden, J. R. Gao, H. Hoever, and T. M. Klapwijk, J. Low Temp. Phys. **151**, 524 (2008).

[12] J. E. Healey, T. Lindstrom, M. S. Colclough, C. M. Muirhead, and A. Y. Tzalenchuk, Appl. Phys. Lett. **93**, 043513 (2008).

[13] W. Chen, D. A. Bennett, V. Patel, and J. E. Lukens, Supercond. Sci. Technol. **21**, 075013 (2008).

[14] A. D. O'Connell, M. Ansmann, R. C. Bialczak, M. Hofheinz, N. Katz, E. Lucero, C. McKenney, M. Neeley, H. Wang, E. M. Weig, A. N. Cleland, and J. M. Martinis, Appl. Phys. Lett. **92**, 112903 (2008).

[15] J. Gao, J. Zmuidzinas, B. A. Mazin, P. K. Day, and H. G. Leduc, Nucl. Instrum. Methods Phys. Res. A **559**, 585 (2006).

[16] See EPAPS supplementary material at http://dx.doi.org/10.1063/1.3273372 for a more detailed discussion of the numerical calculations and relevant parameters.

[17] J. M. Martinis, K. B. Cooper, R. McDermott, M. Steffen, M. Ansmann, K. D. Osborn, K. Cicak, S. Oh, D. P. Pappas, R. W. Simmonds, and C. C. Yu, Phys. Rev. Lett. **95**, 210503 (2005).

[18] G. Stan, S. B. Field, and J. M. Martinis, Phys. Rev. Lett. **92**, 097003 (2004).

[19] C. Song, T. W. Heitmann, M. P. DeFeo, K. Yu, R. McDermott, M. Neeley, J. M. Martinis, and B. L. T. Plourde, Phys. Rev. B **79**, 174512 (2009).